An empirical model for estimating fracture toughness using the DCDC geometry

Christian Nielsen[1], Alireza V. Amirkhizi[2], and Sia Nemat-Nasser[1,*]

[1] *Department of Mechanical and Aerospace Engineering, University of California at San Diego, 9500 Gilman Drive, La Jolla, CA 92093-0416, USA*

[2] *Department of Mechanical Engineering, University of Massachusetts at Lowell, 1 University Avenue, Lowell, MA 01854, USA*

Phone: (858) 534-5930

Fax: (858) 534-2727

Email: sia@ucsd.edu

The double cleavage drilled compression (DCDC) geometry is useful for creating large cracks in a material in a controlled manner. Several models for estimating fracture toughness from DCDC measurements have been proposed, but each is suitable for a subset of geometries and material properties. In this work, a series of finite element fracture simulations are performed over a range of sample widths, hole sizes, heights, Young's moduli, Poisson's ratios, critical stress intensity factors, and boundary conditions. Analyzing the simulation results, fracture toughness is found to be a simple function of sample width, hole size, and an extrapolated stress at zero crack length obtained from a linear fit of the data. Experimental results in the literature are found to agree with this simple relationship.

DCDC, finite element modeling, fracture toughness

1 Introduction

Axial compression is used to drive tensile cracks in the double cleavage drilled compression (DCDC) specimen (Janssen 1974). This interesting fracture behavior results from the specimen geometry transforming the global compression into local regions of tension. The specimen consists of a long rectangular column with a central hole (Fig. 1). Symmetric cracks initiated at the crown and base of the hole propagate along the axis of the specimen in the direction of the applied compression (Horii and Nemat-Nasser 1985). The test is stable when the compression required to grow the cracks increases with crack length. A detailed description of a displacement-controlled DCDC experiment is given by Nielsen et al. (2012).

One of the advantages of the DCDC specimen is that the geometry and boundary conditions will arrest the cracks before they reach the ends of the

specimen. The final specimen remains intact after unloading and contains large axial cracks. This is a desirable configuration, particularly for crack healing studies (Plaisted and Nemat-Nasser 2007), where the sample would otherwise have to be manually reassembled (Chen et al. 2002).

The relationship between the applied compression and the length of the cracks can be used to estimate a material's fracture toughness, and a few models have been proposed. He et al. (1995) generated a linear relationship by fitting the results from linear elastic, plane strain finite element calculations for a variety of DCDC geometries. Nonlinear geometric effects were not considered, meaning the He model is limited to cases with short cracks or very stiff and brittle materials. Analyses using linear geometries cannot include beam-column effects such as buckling. For typical geometries, the He model predicts relatively large increases in axial stress with increases in crack length. This result does not agree with later DCDC experimental observations made by Plaisted et al. (2006) where two distinct regimes of crack growth were observed. After an initial period of increasing axial stress with increasing crack length, a plateau was reached and the cracks continued to grow at an almost constant stress level. Plaisted et al. developed a new, analytical model where the DCDC test is subdivided into short crack and long crack growth regimes. In the short crack growth regime, the sample is treated as a plate with cracks emanating from the central hole using similar assumptions of linear elasticity as He et al. Once the cracks are sufficiently long, the DCDC sample is treated as four beam-columns subjected to bending due to a moment created by the hole and the applied axial compression. As the cracks grow, the lengths of the beams increase. The fracture toughness of the material is related to the induced moment, which is assumed to be constant with crack length in the linear geometry case. The model predicts that crack growth in the long crack growth regime would require a constant stress, a result that nicely fit Plaisted's experimental data. Other experimental results, such as those obtained by Michalske et al. (1993), did not exhibit a similar plateau stress. Adding nonlinear geometric effects to the long crack model is discussed by Plaisted et al. A better estimate of the effective bending moment, particularly as a function of crack length, could improve the model.

We have previously created a finite element simulation scheme to study the DCDC test (Nielsen et al. 2012). The method was originally developed to study

the evolution of the bending moment during the test, but it was determined that fracture toughness could be directly estimated from the output. One quarter of the DCDC geometry is simulated, and the change in internal energy is calculated as the crack is progressively lengthened. The simulation data are correlated with the experimental results to estimate fracture toughness as a function of crack length. This approach is time-consuming. A simple, single-value estimate of fracture toughness would be useful. In the present work, we perform a series of finite element simulations where the DCDC sample hole size, width, length, Young's modulus, Poisson's ratio, critical stress intensity factor, and boundary conditions are systematically varied. The results are used to develop a simple empirical relationship, which can be used to estimate fracture toughness from DCDC experimental results for a range of geometries and material properties.

2 Simulations

The 2D finite element simulation approach previously discussed (Nielsen et al. 2012) was modified to investigate the effect of sample geometry and material properties on the DCDC fracture test. The modified method uses a prescribed critical stress intensity factor to estimate the applied stress as a function of the crack length. Hence, no DCDC experimental data is required as an input for analysis.

One-quarter of the DCDC geometry is modeled (Fig. 1), and the test is simulated for a given crack length, l, using two-dimensional plane stress shell elements, a linear elastic isotropic material model, and considering geometric nonlinearities in the finite element solver. At each displacement step, the crack is virtually grown by one element, and the change in the internal energy, energy release rate, and critical stress intensity factor, K_{Ic}, are calculated. When the simulation K_{Ic} matches the prescribed K_{Ic}, the applied force (stress) at that displacement is associated with the crack length l. Repeating this procedure at successive crack lengths yields a curve of applied stress versus crack length. Table 1 summarizes all of the modeled geometries, material properties, and boundary conditions.

The approach was applied to DCDC experiments on fused silica by Michalske et al. (1993) (Table 1, line 1). The sample geometry and material properties given in the paper were used in the simulation. The critical stress intensity factor of

0.740 MPa·m^{½} had previously been determined by double cantilever beam (DCB) fracture experiments (Weiderhorn et al. 1974). The results of the simulation give stress versus crack length results that closely match the experimentally observed behavior.

The simulation method was also applied to the DCDC experimental geometry and material properties given by Nielsen et al. (2012) (Table 1, line 2). Similar to experimental observations, the computational results show an initial region of increasing stress followed by a plateau region with smaller changes in the fracture stress (Fig. 2 open circles). A period of instability where continued crack growth requires less applied displacement is also observed to initiate at a normalized crack length (l/R) of 6.4. This instability is due to nonlinear geometric effects associated with buckling. No rapid jumps in crack length were noted during the experiments (Nielsen et al. 2012). Reviewing the experimental data, six of the seven samples with cracks that exceeded this critical length show a slight decrease in the applied stress beyond a normalized crack length of ~7. While the simulations considered a linear elastic material, the experiments were conducted on PMMA, a viscoelastic polymer. A non-linear material response, particularly around the hole where the compressive stresses were magnified by the geometry, may have inhibited or masked unstable crack growth during the experiments.

The sample length, width, hole size, critical stress intensity factor, Young's modulus, Poisson's ratio, and displacement boundary condition were varied from the experimental conditions in Nielsen et al. (2012) (Table 1, lines 3-17). Reducing the hole size or width, or increasing the Young's modulus or critical stress intensity factor increases the axial stresses required for crack propagation. Periods of unstable crack growth are observed in most simulations. Increasing the sample length or Young's modulus, reducing the critical stress intensity factor, or having a friction-free boundary condition (e.g. greased loading platens) are found to delay the onset of the instability. The studied Poisson's ratios did not have a significant effect on the results.

3 Estimating fracture toughness

The linear model of He et al. (1996) and the nonlinear model of Plaisted et al. (2006) for estimating K_{Ic} were applied to the axial stress versus crack length simulation results. Generally, the estimates of fracture toughness varied

significantly from the prescribed values, and the overall linear fits were poor. Both models fail to properly capture the slope of the data, with He's empirical model expecting a relatively steep slope and Plaisted's theoretical model expecting a constant plateau stress after a brief initial period with a steep slope. The simulation results generally exhibit an initial period of steep increases in stress followed by a longer period of crack growth with much smaller increases in stress. The slopes of both regimes are affected by the DCDC geometry and material properties.

Inspecting the simulation results, a linear region is apparent during stable long crack growth, typically from approximately l/R=2 to l/R=5. A line was fit to this region in each simulation. The parameters of these lines are given in Table 1. The *y*-intercept of each line, σ_0, appears to only depend on the sample width, hole size, and critical stress intensity factor. Plotting σ_0 as a function of these parameters (Fig. 3 solid squares) gives an approximately linear relationship. A simple model (Fig. 3 line),

$$\frac{K_{Ic}}{\sigma_0\sqrt{w}} = 3\left(\frac{R}{w}\right)^2, \tag{1}$$

is found to closely follow the observed behavior with an R-squared value of 0.998.

4 Comparison with experiments

Published DCDC experimental results (Michalske et al. 1993; Plaisted et al. 2006; Nielsen et al. 2012) were compared with the derived model. The linear fit parameters (m, σ_0) for the experimental data are listed in Table 2, and the σ_0 parameters are plotted as hollow diamonds in Fig. 3. The experimental points follow the same trend observed in the simulation results, although with more deviation from equation (1) (R^2=0.966).

Linear fits of the experimental data from Michalske et al. (1993) and the simulation results for the same geometry and material properties yield fit parameters that straddle the line given by equation (1). The extrapolated stresses at zero crack length derived from the experimental results are 7-8 % less than the σ_0 fit parameter derived from the simulation data. Since the stress versus crack length data from the experiments and simulation are similar for the period of

crack growth where they coincide, the discrepancy could be attributed to the range of data points available for fitting. The minimum crack length of the reported experimental data is l/R=3, while the simulation results were fit between l/R=2 and l/R=5. Having sufficient data points and choosing the appropriate range for fitting are two challenges associated with linear extrapolation and applying equation (1).

Data for PMMA from Plaisted et al. (2006) were grouped by sample geometry, and linear fits were applied to the initial portions of the long crack regimes. The reference critical stress intensity factor was assumed constant and taken as the average of the range determined by Nielsen et al. (2012). The average fit parameter σ_0 from each group of experimental data was compared with equation (1) and generally in good agreement, although two of the geometries show >10 % variation. In the case of the w/R=2 samples, there was a limited number of data points for fitting, which led to wide variation in the fit results.

The experimental results from the DCDC sample thickness study conducted by Nielsen et al. (2012) show an increase in the axial stresses required to propagate long cracks in thicker samples. This translates to an increasing fit parameter σ_0. Since the empirical model, equation (1), was developed using two-dimensional simulations, thickness is not considered, and the associated changes in σ_0 leads to variation in the results. For the assumed K_{Ic} for PMMA, the thinnest samples show the best agreement with the model. This correlates with the conclusion in Nielsen et al. (2012) that the two-dimensional simulations are more applicable to the thinner tested geometries.

5 Conclusions

A series of finite element simulations were used to investigate the effect of sample geometry, material properties, and displacement boundary condition on crack growth behavior during the DCDC fracture test. The linear region of the long crack regime was used to develop a simple estimate of K_{Ic}. While the models given by He et al. (1993) and Plaisted et al. (2006) are applicable to separate, limited ranges of materials and geometries, the empirical model given here was found to give reasonable estimates of K_{Ic} for all considered DCDC cases. A drawback of this model is that the linear region is not always obvious for fitting,

and there is variation in the appropriate range of crack lengths. Care must be taken in applying this model to experimental data. Unstable crack growth can be hard to distinguish from stable growth, as noted for a viscoelastic material like PMMA. Developing a model that includes the slope of the linear fit as a second parameter may be beneficial. The ability to predict the slope of the crack growth behavior in the long crack regime would also be useful for cases where a constant plateau stress is desired (Hamilton et al. 2010).

The model given here was developed empirically and does not illuminate the underlying reasons for the observed behavior. More work is needed to understand these reasons and develop a complete, analytical model.

This work was funded by Air Force Office of Scientific Research grant FA9550-08-1-0314 to UC San Diego.

References

Chen X, Dam MA, Ono K, Mal A, Shen H, Nutt SR, Sheran K, Wudl F (2002) A thermally re-mendable cross-linked polymeric material. Science 295:1698-1702.

Hamilton AR, Sottos NR, White SR (2010) Self-healing of internal damage in synthetic vascular materials. Adv Mater 22:5159-5163.

He MY, Turner MR, Evans AG (1995) Analysis of the double cleavage drilled compression sample for interface fracture energy measurements over a range of mode mixities. Acta Metall et Mater 43:3453-3458.

Horii H, Nemat-Nasser S (1985) Compression-induced microcrack growth in brittle solids: axial splitting and shear failure. J Geophys Res-Sol Ea 90(B4):3105-3125.

Janssen C (1974) Specimen for fracture mechanics studies on glass. 10th Int Congr on Glass: Kyoto, Japan; Ceramic Society of Japan.

Michalske TA, Smith WL, Chen EP (1993). Stress intensity calibration for the double cleavage drilled compression specimen. Eng Fract Mech 45:637-642.

Nielsen C, Amirkhizi AV, Nemat-Nasser S (2012) The effect of geometry on fracture strength measurements using DCDC samples. Eng Fract Mech 91:1-13.

Plaisted TA, Amirkhizi AV, Nemat-Nasser S (2006) Compression-induced axial crack propagation in DCDC polymer samples: experiments and modeling. Int J Fract 141:447-457.

Plaisted TA, Nemat-Nasser S (2007) Quantitative evaluation of fracture, healing and re-healing of a reversibly cross-linked polymer. Acta Mater 55:5684-5696.

Weiderhorn SM, Johnson H, Diness AM, Heuer AH (1974) Fracture of glass in vacuum. J Am Ceram Soc 57:336-341.

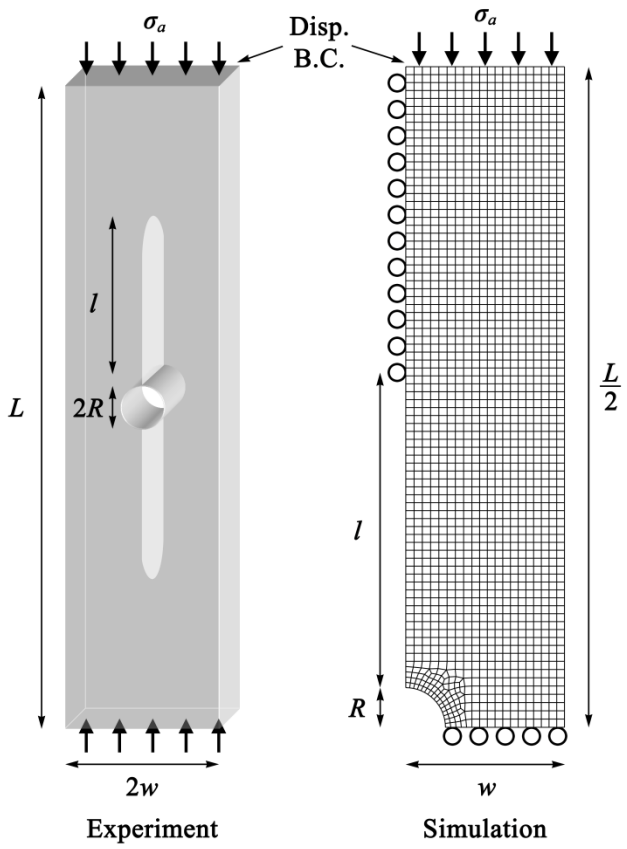

Fig. 1 The DCDC sample geometry for fracture experiments and simulations.

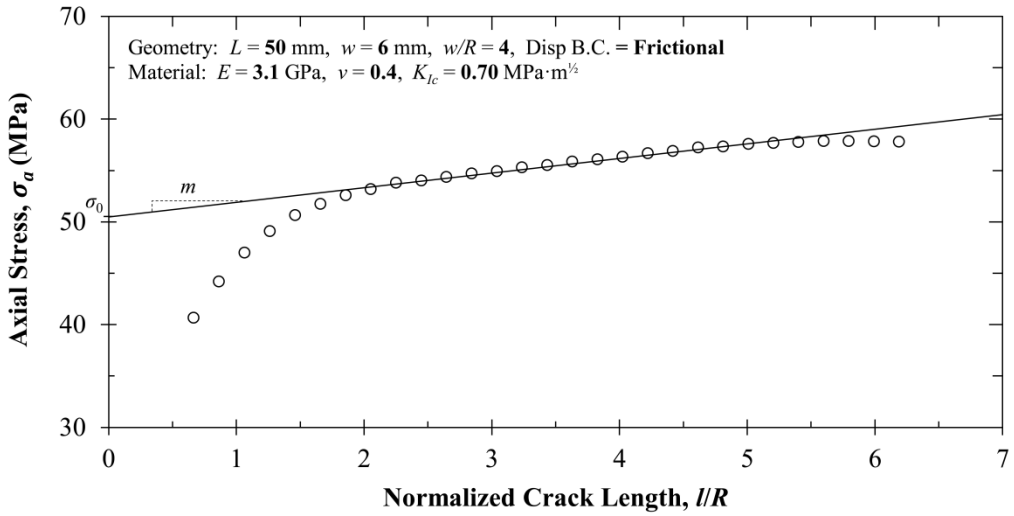

Fig. 2 Simulation results based on the experimental conditions of Nielsen et al. (2012) are plotted (open circles), and the linear region of the long crack regime is fitted (solid line).

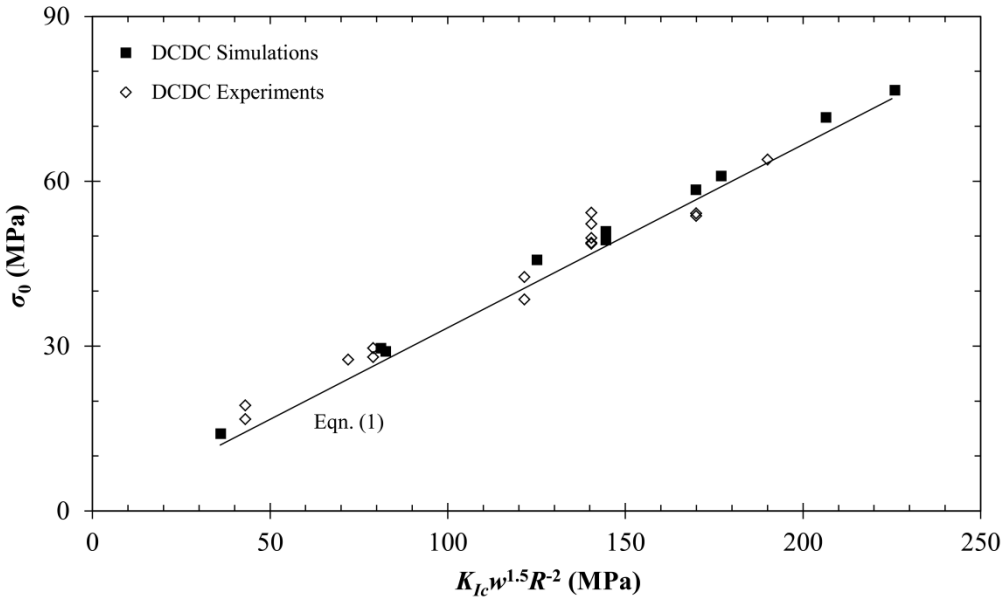

Fig. 3 The simulation results (solid squares), experimental results (open diamonds), and empirical model (solid line) are plotted for comparison.

Table 1 The simulated DCDC geometries, materials properties, and boundary conditions, and linear fits of the corresponding long crack regime. Crack growth in the E=1 GPa case became unstable early in the simulation and a reasonable linear fit could not be made.

Geometry			Material			B.C.	$\sigma_a = m(l/R) + \sigma_0$	
w/R	w (mm)	L (mm)	E (GPa)	K_{Ic} (MPa·m^{½})	v		m	σ_0 (MPa)
3.75	3.75	75	73	0.740	0.17	Frictional	5.7273	58.366
4	6	50	3.1	0.7	0.4	Frictional	1.4215	50.490
2	6	50	3.1	0.7	0.4	Frictional	0.8289	14.028
3	6	50	3.1	0.7	0.4	Frictional	1.3344	29.582
5	6	50	3.1	0.7	0.4	Frictional	1.1400	76.475
4	4	50	3.1	0.7	0.4	Frictional	1.4787	60.892
4	8	50	3.1	0.7	0.4	Frictional	0.0055	45.644
4	6	30	3.1	0.7	0.4	Frictional	0.3995	47.311
4	6	100	3.1	0.7	0.4	Frictional	1.7500	49.259
4	6	50	1	0.7	0.4	Frictional	-	-
4	6	50	10	0.7	0.4	Frictional	3.3126	50.342
4	6	50	73	0.7	0.4	Frictional	4.3675	49.976
4	6	50	3.1	0.4	0.4	Frictional	1.4244	28.948
4	6	50	3.1	1.0	0.4	Frictional	0.9059	71.561
4	6	50	3.1	0.7	0.3	Frictional	1.4911	50.177
4	6	50	3.1	0.7	0.495	Frictional	1.3537	50.792
4	6	50	3.1	0.7	0.4	Friction-free	1.7738	49.676

Table 2 The experimental DCDC geometries, material properties, and boundary conditions, and linear fits of the corresponding long crack regimes.

Data Source	Geometry				Material			B.C.	$\sigma_a = m(l/R) + \sigma_0$	
	w/R	w (mm)	L (mm)	t (mm)	E (GPa)	K_{Ic} (MPa·m^{½})	v		m	σ_0 (MPa)
[1]	3.75	3.75	75	6.5	73	0.740	0.17	Frictional	6.6878	54.112
[1]	3.75	3.75	75	6.5	73	0.740	0.17	Frictional	6.5426	53.664
[2]	2	4	50	11	3.1	0.68	0.4	Frictional	0.9795	19.178
[2]	2	4	50	11	3.1	0.68	0.4	Frictional	0.9795	19.178
[2]	2	4	100	11	3.1	0.68	0.4	Frictional	2.4303	16.697
[2]	3	6	50	11	3.1	0.68	0.4	Frictional	0.7495	29.607
[2]	3	6	100	11	3.1	0.68	0.4	Frictional	0.6237	27.959
[2]	3	8	100	11	3.1	0.68	0.4	Frictional	0.5890	27.525
[2]	4	8	50	11	3.1	0.68	0.4	Frictional	1.0554	42.561
[2]	4	8	100	11	3.1	0.68	0.4	Frictional	0.5155	38.488
[3]	5	8	50	11	3.1	0.68	0.4	Frictional	1.1592	63.895
[3]	4	6	50	3	3.1	0.68	0.4	Frictional	0.8603	48.793
[3]	4	6	50	4	3.1	0.68	0.4	Frictional	0.9449	48.600
[3]	4	6	50	5	3.1	0.68	0.4	Frictional	0.9386	49.628
[3]	4	6	50	8	3.1	0.68	0.4	Frictional	0.6409	52.228

[1] Michalski et al. 1993

[2] Plaisted et al. 2006

[3] Nielsen et al. 2012